ChemPubSoc Europe

DOI: 10.1002/cphc.201402819

CHEMPHYSCHEM Communications

Entropic Separations of Mixtures of Aromatics by Selective Face-to-Face Molecular Stacking in One-Dimensional Channels of Metal–Organic Frameworks and Zeolites

Ariana Torres-Knoop,*[a] Salvador R. G. Balestra,[b] Rajamani Krishna,[a] Sofía Calero,[b] and David Dubbeldam[a]

Separation of challenging mixtures using metal–organic frameworks can be achieved by an entropy-driven mechanism, where one of the components can arrange into a "face-to-face" stacking, thus reducing its "footprint" and reaching a higher saturation loading.

Exploiting and understanding separation mechanisms that are effective at pore saturation conditions is of crucial importance to design and develop next-generation nanoporous materials for industrial applications. In this paper, we elucidate a new selectivity mechanism based on the reorientation of a selected component into a "face-to-face" stacking arrangement. With increased loading, that component can significantly reduce its "footprint" with respect to the other components and hence obtain a higher saturation loading. Using state-of-the-art molecular simulations we explore the underlying mechanism behind this reorientation. We highlight the hitherto unrealized potential of the entropy based separation for mixtures of C8 hydrocarbons by showing how this mechanism leads to *o*-xylene and benzene selectivity in AFI and MAZ zeolite. We also demonstrate that 1,3,5-trichlorobenzene can be selectively adsorbed from its isomers due to its optimal face-to-face stacking within the triangular channels of a $Fe_2(BDP)_3$ variant.

Nanoporous materials such as zeolites, metal–organic frameworks (MOFs), and zeolitic imidazolate frameworks (ZIFs) offer considerable potential as energy-efficient alternatives to conventional separation processes like distillation, absorption, and extraction. Separation in nanoporous materials relies on adsorption and/or diffusion properties and can be achieved by size/shape exclusion (steric separation), by differences in the adsorbate-adsorbent interactions and/or adsorbate packing interactions (thermodynamic equilibrium effect) or by differences in the diffusion rate of the adsorbates within the adsorbent channels.

[a] *A. Torres-Knoop, Prof. Dr. R. Krishna, Dr. D. Dubbeldam*
Van 't Hoff Institute for Molecular Sciences
University of Amsterdam
Science Park 904, 1098 XH Amsterdam (The Netherlands)
E-mail: A.TorresKnoop@uva.nl

[b] *S. R. G. Balestra, Prof. Dr. S. Calero*
Department of Physical, Chemical and Natural Systems
University Pablo de Olavide
Ctra. Utrera km. 1, 41013 Sevilla (Spain)

Supporting Information for this article is available on the WWW under http://dx.doi.org/10.1002/cphc.201402819.

At low loadings (i.e. the Henry regime), adsorbate–adsorbate interactions are of little importance. The selectivity is mainly driven by enthalpic effects, and is in favor of the molecule that has the strongest interaction with the framework. This is the principle behind most separations of mixtures of light gaseous compounds, where a common feature is that saturation conditions are often not reached. For example, the selective adsorption of CO_2 from mixtures containing N_2, H_2, CO, and CH_4 by selective binding of CO_2 with either the metal atoms (M) of CuBTC,[1] Cu-TDPAT,[2] M-MOF-74[3,4] or the extra-framework cations of NaX zeolite[5] and the selective adsorption of N_2 from O_2 based on the larger quadrupole moment of N_2 in both LTA-4 A and LTA-5 A.[6]

However, many industrially used setups operate close to saturation conditions, for example, liquid-phase adsorption. At these conditions, adsorption is dominated by entropic effects and therefore highly influenced by adsorbate–adsorbate interactions and packing efficiency. Up to date, several entropy effects have been discovered and exploited for mixture separations: 1) size entropy, 2) configurational entropy, 3) commensurate stacking, and 4) length entropy.

"Size entropy" effects arise from the fact that smaller molecules can fit easier in the "gaps" between adsorption sites, leading to higher saturation capacities with decreasing molecules size. An example is the separation of alkanes in MFI.[7] "Configurational entropy" effects favor molecules with better packing within the pores structure. The length and topology of one of the mixture components is comparable with the channels leading to "commensurate freezing".[8] This is the case in the separation of linear from branched alkanes in silicalite-1, where the linear n-hexane (nC6) is favored over the dibranched isomers 2,2-dimethylbutane (22DMB) and 2,3-dimethylbutane (23DMB).[9–11] "Commensurate stacking" occurs when the packing arrangement of one of the components is commensurate with the channel size, which allows this component to stack like books on a bookshelf. This is observed in the adsorption of *o*-xylene in MIL-47 and *p*-xylene in MAF-x8.[12] "Length entropy" effects favor molecules with the shortest length (footprint) in one-dimensional channels, since they can be pack more efficiently within the channels. A good example is the separation of hexane isomers in AFI channels, where selectivity relies on the smaller footprints of the branched isomers 22DMB and 23DMB.[13–15]

In this article, we describe a new entropy-based separation mechanism in one-dimensional channels at saturation capacity. In this mechanism, the selectivity relies on a loading-driven re-

orientation of one of the mixture components into a 'pile' configuration where all the molecules are in a "face-to-face" orientation. We demonstrate this effect in two systems: 1) *o*-xylene and benzene in AFI and MAZ zeolite channels (which can be efficiently separated from *m*-, *p*-xylene and ethylbenzene), and 2) 1,3,5-trichlorobenzene in a triangular MOF (which can be efficiently separated from 1,2,4-/1,2,3-trichlorobenzene).

AFI zeolite possesses one-dimensional channels with corrugated pore topology; the channel diameter at the narrow constrictions is 7.3 Å, and at the protracted segments it is 8.4 Å. MAZ zeolite is slightly smaller than AFI; the channel diameters at the narrow and protracted segments are 6.7 and 7.4 Å, respectively. Figure 1 shows snapshots of benzene, *o*-, *p*-, *m*-xylene and ethylbenzene at saturation loading. The height and wide of *o*-xylene and benzene are both smaller than 8.4 and 7.4 Å, allowing a perpendicular alignment (with respect to the channel axis) within the protracted channel segments in both AFI and MAZ. For *m*-, *p*-xylene and ethylbenzene, either the height or width, is too large to allow vertical alignment; consequently their orientations within the channels are aligned obliquely.

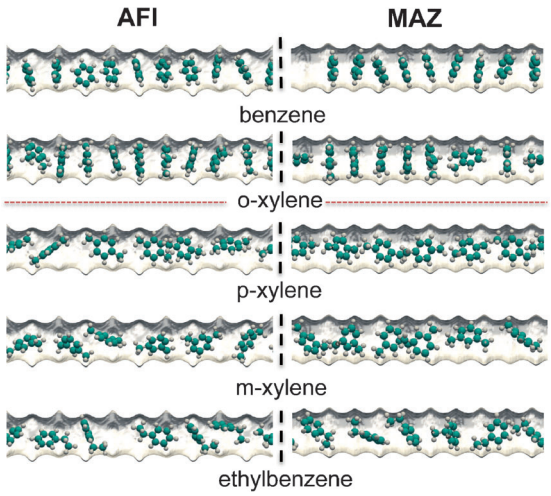

Figure 1. Snapshots of benzene, *o*-, *p*- and *m*-xylene and ethylbenzene in AFI (left) and MAZ (right) channels at saturation conditions. Benzene and *o*-xylene are able to change their orientation from parallel to perpendicular (relative to the channel axis). At high loadings, this leads to a "face-to-face" arrangement that reduces their "footprint" compared to *p*- and *m*-xylene and ethylbenzene.

Because of the perpendicular alignment, *o*-xylene and benzene reduce their effective footprint and achieve much higher saturation capacities, as shown in Figure S1 of the Supporting Information (SI), where configurational-bias continuous fractional component Monte Carlo (CB/CFCMC) simulations[16] of pure-component isotherms for hydrocarbons in AFI at 433 K are presented. The simulations are in very good qualitative agreement with the experimental data (at 303 K) of Chiang et al.[17] and provide the means to understand why. For MAZ zeolite the simulation results show the same difference in saturation capacity between adsorbates that can change their orientation compared to those that cannot (Figure S2). In MAZ, however, a difference between benzene and *o*-xylene shows up that is not present in AFI. This is because MAZ is slightly smaller than AFI and although *o*-xylene is able to align perpendicular, the tighter confinement does not allow for a complete "face-to-face" stacking at this range of pressures. This suggests that a 1D channel slightly smaller than MAZ would be perfect to separate benzene from other aromatics. Benzene is the main precusor for ethylbenzene, cumene and cyclohexane, use for the production of styrene/polystyrene, resins and Nylon.

In Figure 2, we show the CB/CFCMC simulation isotherms (inset) and the simulated breakthroughs at 100 kPa for an equimolar mixture of *o*-xylene/*p*-xylene/*m*-xylene/ethylbenzene in AFI at 433 K. The CB/CFCMC mixture simulations for the four-component mixture are in excellent agreement with the IAST calculations based on pure-component isotherms fits (fit parameters are provided in the SI). The isotherms clearly show AFI selectivity for *o*-xylene at saturation conditions. The sequence of breakthroughs shows that the breakthrough of *o*-xylene occurs significantly later than that of ethylbenzene and *p*- and *m*-xylene. This ensures a highly selective separation of *o*-xylene from the other components and demonstrates the possibility of separation of a four-component *o*-xylene/*m*-xylene/*p*-xylene/ethylbenzene mixture on the basis of molecules reorientation provided pore saturation conditions are attained. Our results are in good agreement with Hu et al.[18,19] transient breakthrough experiments.

The experimental results of Chiang et al.[17] already suggest that benzene and *o*-xylene arrange in a "face-to-face" configuration in AFI. By dividing the loading per channel by the channel length it is clear that the footprint of the molecules is

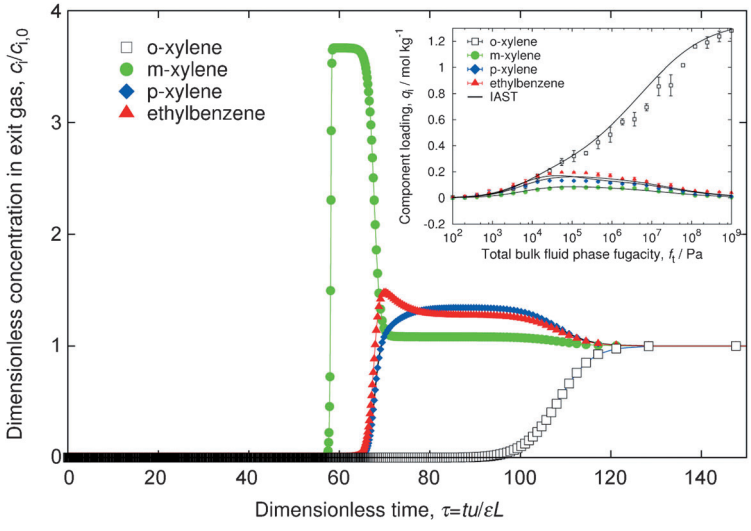

Figure 2. Breakthroughs simulation at 100 kPa and mixture isotherms (inset) for an equimolar mixture of *o*-xylene/*p*-xylene/*m*-xylene/ethylbenzene in AFI zeolite at 433 K. The breakthrough simulation methodology is the same as that used in our earlier work.[12] Video animations showing the breakthrough of a four-component aromatics mixture in AFI zeolite has been included as SI. The reorientation of *o*-xylene allows a higher saturation capacity and drives the other mixture components out of the AFI zeolite. This makes AFI an *o*-xylene-selective structure. Diffusion considerations do not change this.

small, but the experimental data is insufficient to elucidate how and why. Chiang et al. purported that even at low loading, benzene molecules would prefer to be orientated perpendicular in AFI. But this is not the case. It is not an energetic, but an entopic effect. We note that perpendicular alignments of aromatics have been observed before by Lucena et al.[20,21] in AEL and AFI zeolite and by Rungsirisakun et al.[22] in MFI (ZSM-5 type).

To investigate and elucidate the molecular mechanism, we measured the distribution of the angle between the aromatic ring plane of *o*-xylene and the channel axis of AFI at different loadings. In Figure 3, the data is presented in a form where

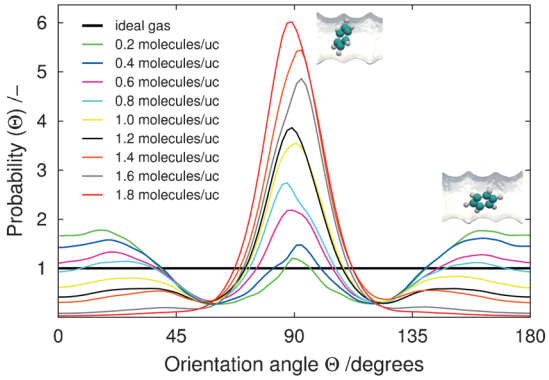

Figure 3. Distribution of the angle between the aromatic ring of *o*-xylene and the channel axis of AFI at 433 K for different loadings. As loading increases, the molecules orient with the aromatic ring perpendicular to the channel axis (90°). The flat black line represents the distribution of an ideal gas.

a horizontal line corresponds to no preferred orientation (as occurs in an ideal gas). We observe that at low loadings, the preferred orientation of the molecules is parallel to the channel axis (0,180°). This orientation was further confirmed by energy minimizations. As the loading increases, adsorbate–adsorbate interactions come into play and the distribution of the orientation of the molecules changes. Adsorbates start to confine each other, and if the loading is increased, the *o*-xylene adsorbates are more and more often found in the perpendicular orientation (90°), leading to a pile of molecules. The reorientation of *o*-xylene into a pile reduces its footprint within the AFI channels and therefore higher saturation capacities are obtained. The mechanism could be viewed as a footprint-entropy effect where the footprint entropy is now strongly loading dependent and changed by a favorable reorientation of the molecule.

We found that the effect is not caused by the corrugation of the wall. Even without walls (in simulations we achieve this by omitting the framework and instead restrict the molecules to a volume and shape corresponding to a channel), the effect can be observed. Also, the effect is largely independent of the molecular properties at the Henry regime. A weaker adsorbing molecule that is able to reorient wins at saturation from a stronger adsorbate that is unable to reorient. This is the case of benzene in AFI and MAZ zeolite. In both cases, benzene has a higher saturation capacity than *p*-xylene, *m*-xylene or ethylbenzene, but a lower heat of adsorption (Figure S3).

A class of molecules that have a reduced footprint by reorientation are aromatics, but the effect should be applicable to any adsorbate with one dimension significantly smaller than the other two. The effect is also not limited to the smallest molecules in a mixture. If the larger molecule is (when reoriented) close to the dimensions and shape of the channel and able to change its orientation, but the smallest is not, then the largest molecule will be both entropically and energetically favored at saturation conditions.

As an example on how to exploit the reorientation, we predicted the separation of 1,3,5-trichlorobenzene from its isomers based on the reorientation into a pile configuration of this isomer in a modified $Fe_2(BDP)_3$ metal–organic framework. In the modified structure, the BDP linkers (BDP^{2-} = 1,4-benzenedipyrazolate) were substituted by 4,4′- bis(1H-pyrazol-4-yl) biphenyl linkers[23] to increase the channel size (Figure S4). Figure 4 shows that the small differences in the isomers shape

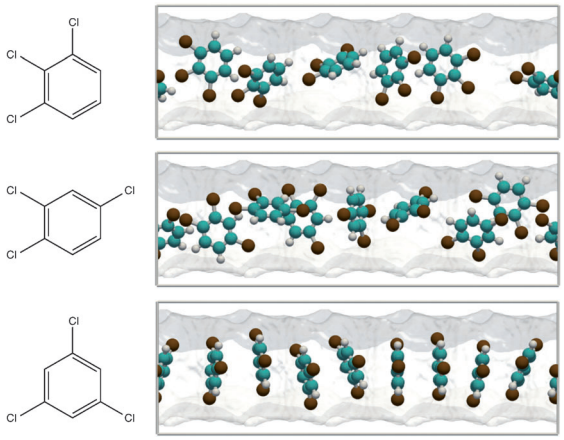

Figure 4. Snapshots of trichlorobenzene isomers in $Fe_2(BDP)_3$ variant. Only 1,3,5-trichlorobenzene is able to reorient into a pile configuration. This reorientation reduces the footprint of the molecule and permits a higher saturation capacity. Color code: carbon (cyan), chlorine (brown), hydrogen (white).

are enough to only permit the 1,3,5-trichlorobenzene to reorient and reduce its footprint within the channels, allowing this isomer to reach a higher saturation capacity (Figure S5). In Figure 5, the CB/CFCMC simulated mixture isotherms of an equimolar mixture of trichlorobenzene isomers are presented. The reorientation into a pile of 1,3,5-trichlorobenzene leads to a very efficient separation, especially under saturation conditions.

When in a mixture of components only one of them has the right size to rotate inside the channels, this mechanism can lead to important differences in saturation capacities. Therefore, highly selective separations can be achieved by the proper choice of one-dimensional channel sizes at saturation conditions. Our CB/CFCMC and breakthrough simulations clearly underscore the potential of adopting separation strategies that rely on differences in molecular footprints, rather than adsorption strengths.

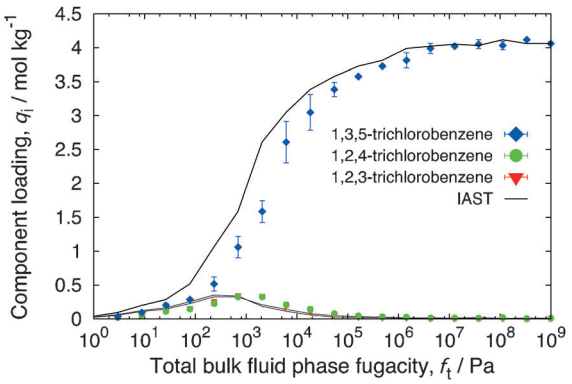

Figure 5. Mixture isotherms for a 1,3,5-/1,2,4-/1,2,3-trichlorobenzene equimolar mixture in the modified $Fe_2(BDP)_3$ structure at 433 K. Molecules that are able to reorient into a "face-to-face" configuration have higher saturation capacities. Differences in the saturation capacities have a strong influence on the separation performance.

Acknowledgements

This work was supported by the Netherlands Organization for Scientific Research/Chemical Sciences (NWO/CW) through a VIDI grant (D. Dubbeldam) and by the European Research Council (ERC) through a Starting Grant ERC-2011-StG-279520-RASPA (S. Calero).

Keywords: aromatic compounds · entropy · mixtures · MOFs · separation

[1] L. Hamon, E. Jolimaître, G. D. Pirngruber, *Ind. Eng. Chem. Res.* **2010**, *49*, 7497 – 7503.
[2] H. Wu, K. Yao, Y. Zhu, B. Li, Z. Shi, R. Krishna, J. Li, *J. Phys. Chem. C* **2012**, *116*, 16609 – 16618.
[3] J. A. Mason, K. Sumida, Z. R. Herm, R. Krishna, J. R. Long, *Energy Environ. Sci.* **2011**, *4*, 3030 – 3040.
[4] Z. R. Herm, J. A. Swisher, B. Smit, R. Krishna, J. R. Long, *J. Am. Chem. Soc.* **2011**, *133*, 5664 – 5667.
[5] Y. Belmabkhout, G. Pirngruber, E. Jolimaitre, A. Methivier, *Adsorption* **2007**, *13*, 341 – 349.
[6] R. Krishna, *Microporous Mesoporous Mater.* **2014**, *185*, 30 – 50.
[7] F. Kapteijn, J. A. Moulijn, R. Krishna, *Chem. Eng. Sci.* **2000**, *55*, 2923 – 2930.
[8] B. Smit, T. Maesen, *Nature* **1995**, *374*, 42 – 44.
[9] T. J. H. Vlugt, R. Krishna, B. Smit, *J. Phys. Chem. B* **1999**, *103*, 1102 – 1118.
[10] R. Krishna, B. Smit, T. H. J. Vlugt, *J. Phys. Chem. A* **1998**, *102*, 7727 – 7730.
[11] T. Titze, C. Chmelik, J. Kärger, J. M. van Baten, R. Krishna, *J. Phys. Chem. C* **2014**, *116*, 2660 – 2665.
[12] A. Torres-Knoop, R. Krishna, D. Dubbeldam, *Angew. Chem. Int. Ed.* **2014**, *53*, 7774 – 8.
[13] J. M. van Baten, R. Krishna, *Microporous Mesoporous Mater.* **2005**, *84*, 179 – 191.
[14] R. Krishna, B. Smit, S. Calero, *Chem. Soc. Rev.* **2002**, *31*, 185 – 194.
[15] R. Krishna, J. M. van Baten, *Phys. Chem. Chem. Phys.* **2011**, *13*, 10593 – 10616.
[16] A. Torres-Knoop, S. P. Balaji, T. H. J. Vlugt, D. Dubbeldam, *J. Chem. Theory Comput.* **2014**, *10*, 942 – 952.
[17] A. S. T. Chiang, C. K. Lee, Z. H. Chang, *Zeolites* **1991**, *11*, 380.
[18] E. Hu, A. T. Derebe, K. Wang, *Int. Journal Materials Sci. Eng.* **2014**, *2*, 10 – 14.
[19] E. Hu, Z. Lai, K. Wang, *J. Chem. Eng. Data* **2010**, *55*, 3286 – 3289.
[20] S. M. P. Lucena, R. Q. Snurr, C. L. Cavalcante Jr., *Adsorption* **2007**, *13*, 477 – 484.
[21] S. M. P. Lucena, J. A. F. R. Pereira, C. L. Cavalcante Jr., *Microporous and Mesoporous Mater.* **2006**, *88*, 135 – 144.
[22] R. Rungsirisakun, T. Nanok, M. Probst, J. Limtrakul, *J. Mol. Graphics Modell.* **2006**, *24*, 373 – 382.
[23] N. Masciocchi, S. Galli, V. Colombo, A. Maspero, G. Palmisano, B. Seyyedi, C. Lamberti, *J. Am. Chem. Soc.* **2010**, *132*, 7902 – 7904.

Received: November 19, 2014
Published online on December 11, 2014

CHEMPHYSCHEM

Supporting Information

Entropic Separations of Mixtures of Aromatics by Selective Face-to-Face Molecular Stacking in One-Dimensional Channels of Metal–Organic Frameworks and Zeolites

Ariana Torres-Knoop,*[a] Salvador R. G. Balestra,[b] Rajamani Krishna,[a] Sofía Calero,[b] and David Dubbeldam[a]

cphc_201402819_sm_miscellaneous_information.pdf
cphc_201402819_sm_1.mov
cphc_201402819_sm_2.mov

Supporting Information to accompany:

Entropic Separations of Mixtures of Aromatics by Selective Face-to-Face Molecular Stacking in One-Dimensional Channels of Metal-Organic Frameworks and Zeolites

1

Single component isotherms in AFI zeolite at 433K

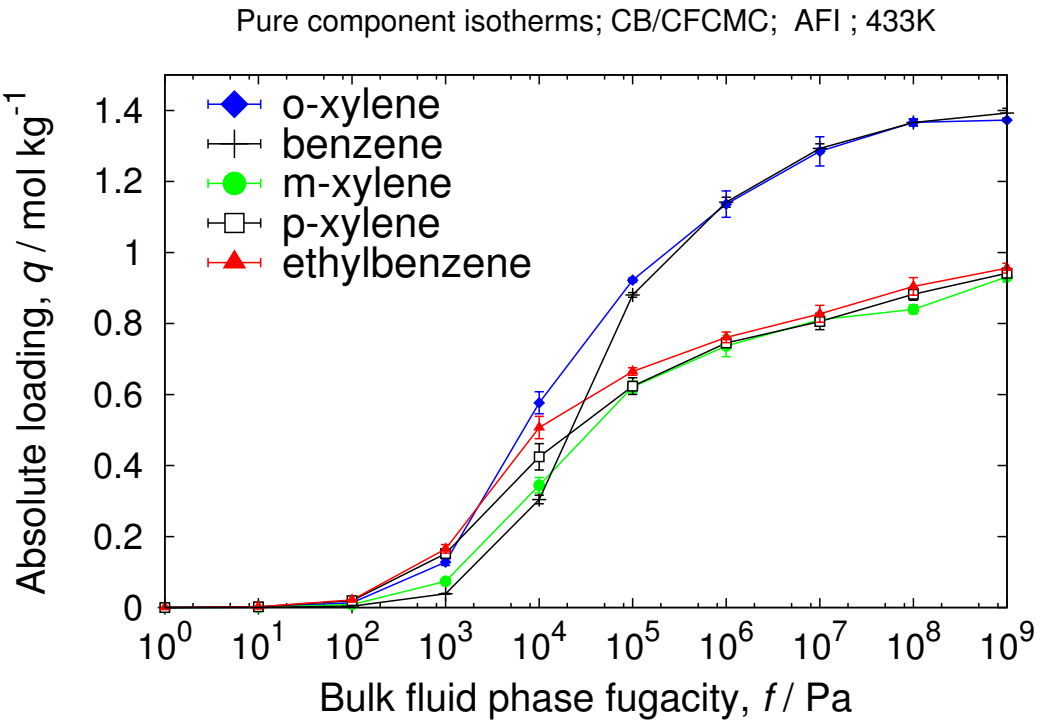

Figure S1: *Single component isotherms in AFI zeolite at 433K. At saturation conditions, benzene and o-xylene can reach higher loadings because of molecular reorientation. This can be exploited as a separation mechanism in liquid conditions.*

2

Single component isotherms in MAZ zeolite at 433K

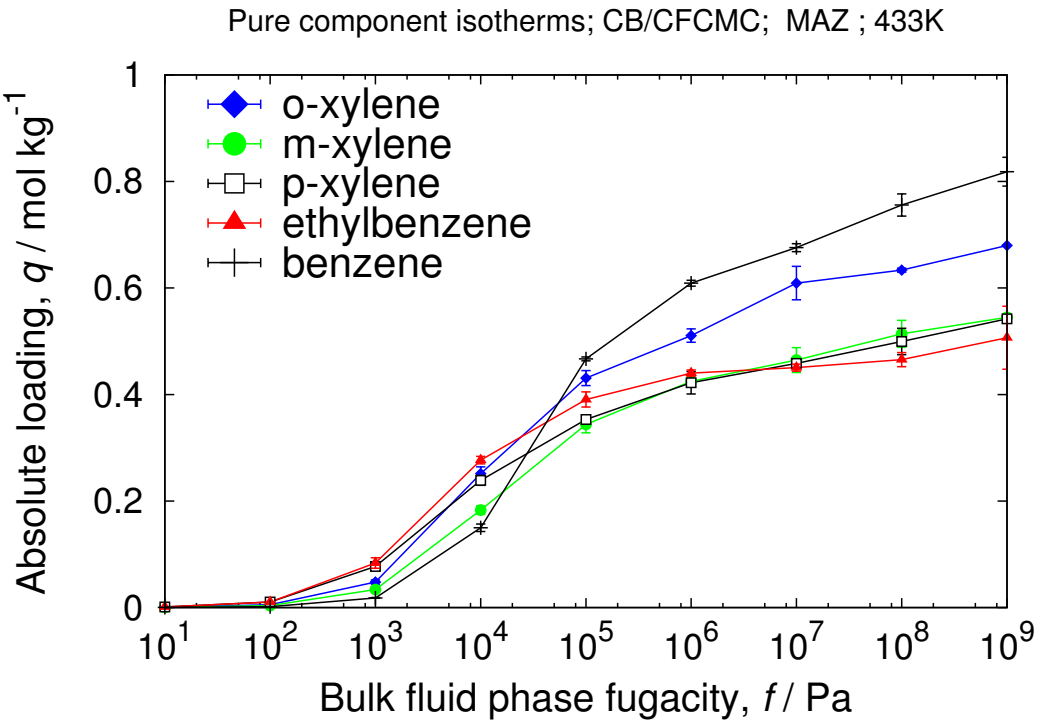

Figure S2: *Single component isotherms in MAZ zeolite at 433K. The smaller channel of MAZ compared to AFI allows for a better reorientation of benzene.*

3

Heat of adsorption in AFI and MAZ zeolite

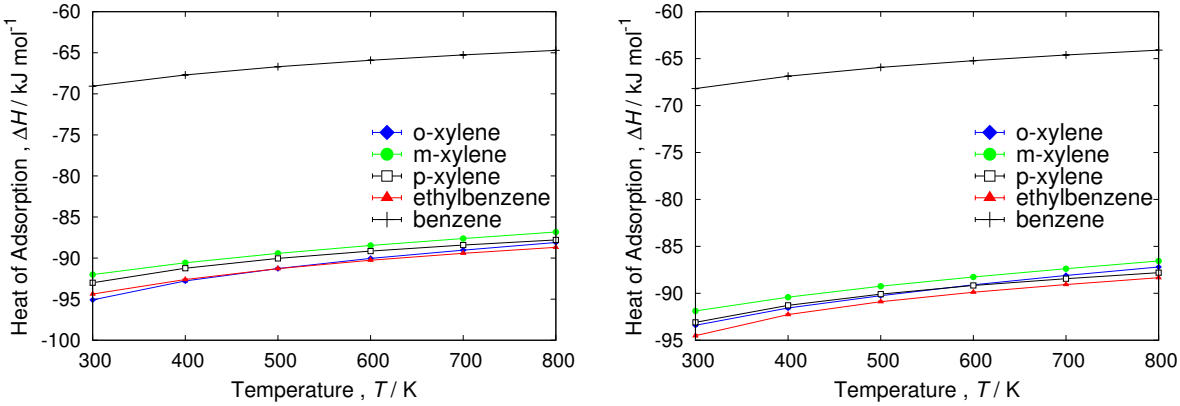

Figure S3: *Infinite dilution heat of adsorption of benzene, o-, m-, p-xylene and ethylbenzene in AFI (left) and MAZ (right) zeolites at different temperatures. For AFI zeolite, our results agree qualitatively with the experimental results of Chiang et al. [1]. In the Henry regime, benzene is the least strongly adsorbed species in both zeolites.*

4

Langmuir-Freundlich parameters for pure component aromatics at 433K in AFI

	site A			site B		
	$q_{i,A,\text{sat}}$ [molec. uc^{-1}]	$b_{i,A}$ [Pa$^{-\nu_{i,A}}$]	$\nu_{i,A}$ [-]	$q_{i,B,\text{sat}}$ [molec. uc^{-1}]	$b_{i,B}$ [Pa$^{-\nu_{i,B}}$]	$\nu_{i,B}$ [-]
o-xylene	0.402	7.63×10^{-7}	1	0.957	1.5×10^{-4}	1
m-xylene	0.208	1.26×10^{-7}	1	0.6935	0.6935×10^{-4}	1
p-xylene	0.277	5×10^{-7}	1	0.624	0.624×10^{-4}	1
ethylbenzene	0.208	3.18×10^{-7}	1	0.6935	0.6935×10^{-4}	1
benzene	0.2635	1.94×10^{-7}	1	1.123	1.123×10^{-5}	1
toluene	0.444	4.15×10^{-7}	1	0.929	0.929×10^{-5}	1

Table S1: *Dual-site Langmuir-Freundlich parameters for pure component xylene isomers at 433 K in AFI. The saturation capacities are expressed in molecules per unit cell; these numbers need to be multiplied by the conversion factor of 1.082 to get mol kg^{-1}.*

$$q_i = q_{i,A,sat} \frac{b_{i,A} f_i^{\nu_{i,A}}}{1 + b_{i,A} f_i^{\nu_{i,A}}} + q_{i,B,sat} \frac{b_{i,B} f_i^{\nu_{i,B}}}{1 + b_{i,B} f_i^{\nu_{i,B}}} \tag{4.1}$$

5

$Fe_2(BDP)_3$ variant

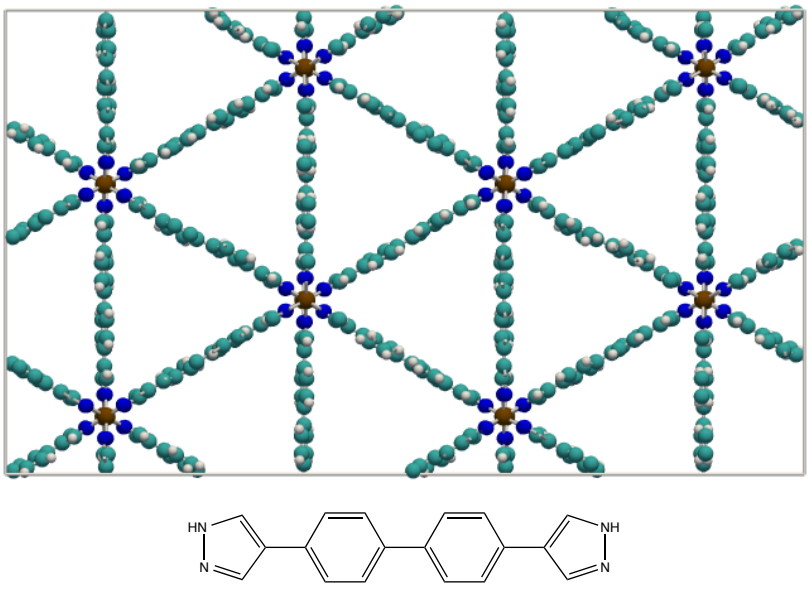

Figure S4: *$Fe_2(BDP)_3$ variant with a $4,4'-bis(1H-pyrazol-4-yl)$biphenyl instead of a BDP linker. The topology of the metal organic framework is the same as the $Fe_2(BDP)_3$, triangular 1D channels running in the z-direction, but the size of the channels is larger due to the extra aromatic molecule in the linker. Color code: organic linker (cyan), iron (brown), nitrogen (blue).*

6

Single component isotherms of trichlorobenzene isomers

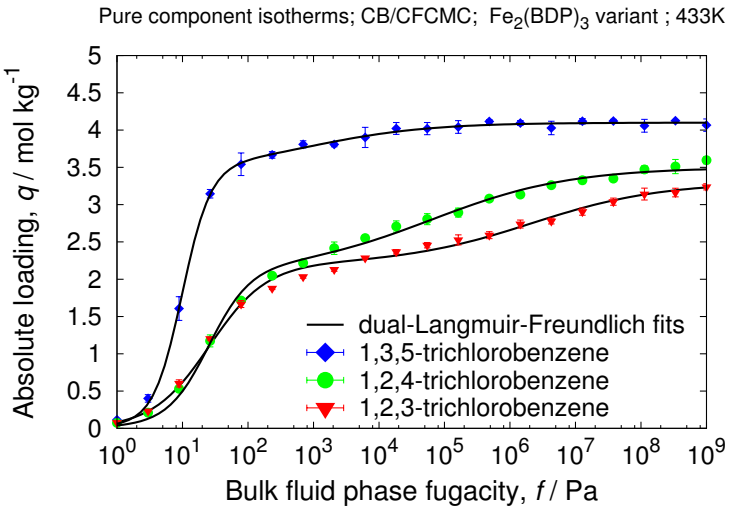

Figure S5: *Single component isotherms of 1,3,5-/1,2,4- and 1,2,3-trichlorobenzene in $Fe_2(BDP)_3$ variant at 433K. The 1,3,5-trichlorobenzene is the only isomer that can reorient within the metal-organic framework channels, which permits a higher saturation capacity.*

	site A			site B		
	$q_{i,A,\text{sat}}$ [mol. kg^{-1}]	$b_{i,A}$ [Pa$^{-\nu_{i,A}}$]	$\nu_{i,A}$ [-]	$q_{i,B,\text{sat}}$ [mol. kg^{-1}]	$b_{i,B}$ [Pa$^{-\nu_{i,B}}$]	$\nu_{i,B}$ [-]
1,3,5	3.45	1.03×10^{-2}	2	0.65	4.3×10^{-2}	0.47
1,2,4	1.4	1.07×10^{-2}	0.41	2.1	2.1×10^{-2}	1.38
1,2,3	1.1	1.64×10^{-3}	0.44	2.2	2.2×10^{-2}	1

Table S1: *Dual-site Langmuir-Freundlich parameters for pure component trichlorobenzene isomers at 433 K in $Fe_2(BDP)_3$ variant. The saturation capacities are expressed in mol kg^{-1}*

Bibliography

[1] A.S.T. Chiang, C.K. Lee, and Chang Z. H. *Zeolites*, 11:380, 1991.

CHEMPHYSCHEM

Supporting Information

Entropic Separations of Mixtures of Aromatics by Selective Face-to-Face Molecular Stacking in One-Dimensional Channels of Metal–Organic Frameworks and Zeolites

Ariana Torres-Knoop,*[a] Salvador R. G. Balestra,[b] Rajamani Krishna,[a] Sofía Calero,[b] and David Dubbeldam[a]

cphc_201402819_sm_miscellaneous_information.pdf
cphc_201402819_sm_1.mov
cphc_201402819_sm_2.mov

Supporting Information to accompany:

Entropic Separations of Mixtures of Aromatics by Selective Face-to-Face Molecular Stacking in One-Dimensional Channels of Metal-Organic Frameworks and Zeolites

1

Single component isotherms in AFI zeolite at 433K

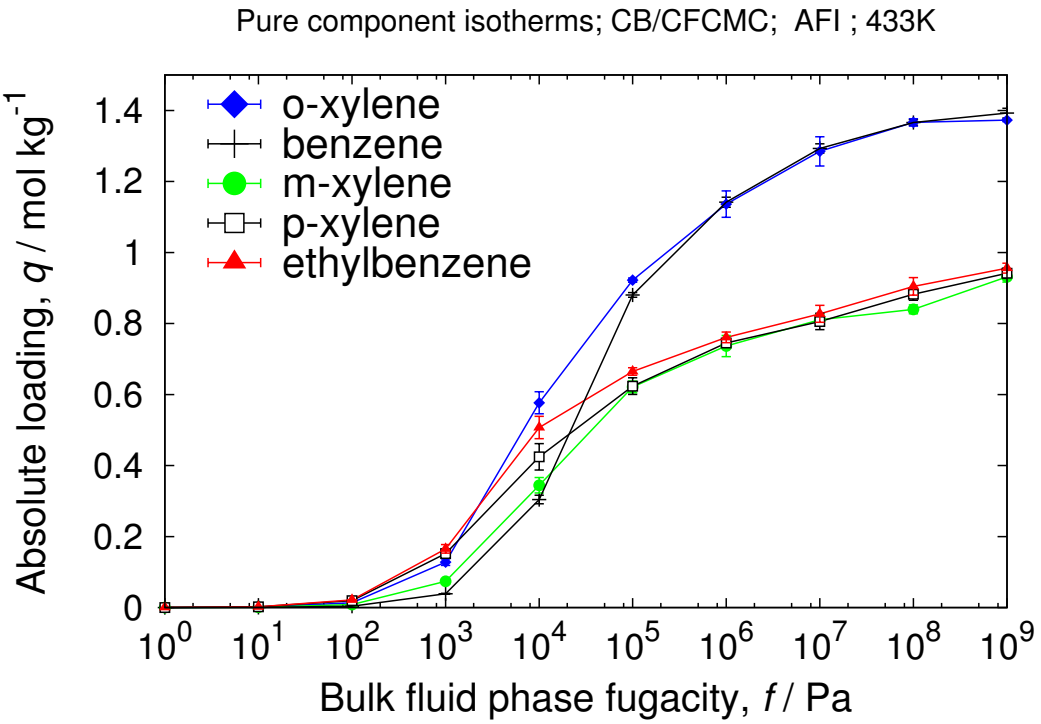

Figure S1: *Single component isotherms in AFI zeolite at 433K. At saturation conditions, benzene and o-xylene can reach higher loadings because of molecular reorientation. This can be exploited as a separation mechanism in liquid conditions.*

2

Single component isotherms in MAZ zeolite at 433K

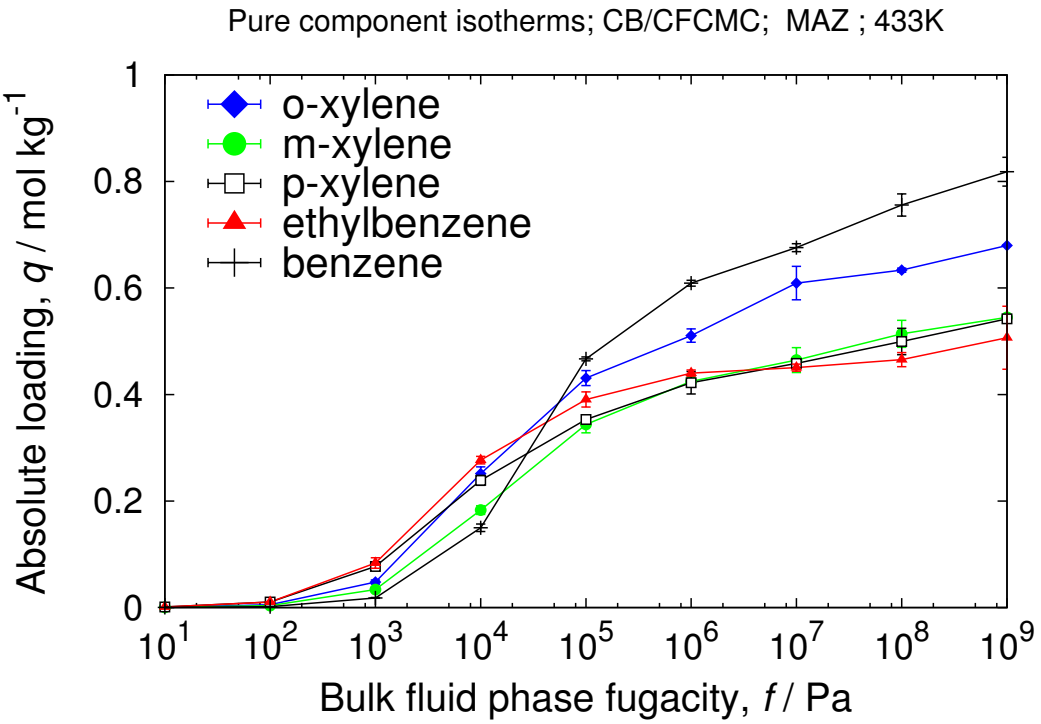

Figure S2: *Single component isotherms in MAZ zeolite at 433K. The smaller channel of MAZ compared to AFI allows for a better reorientation of benzene.*

3

Heat of adsorption in AFI and MAZ zeolite

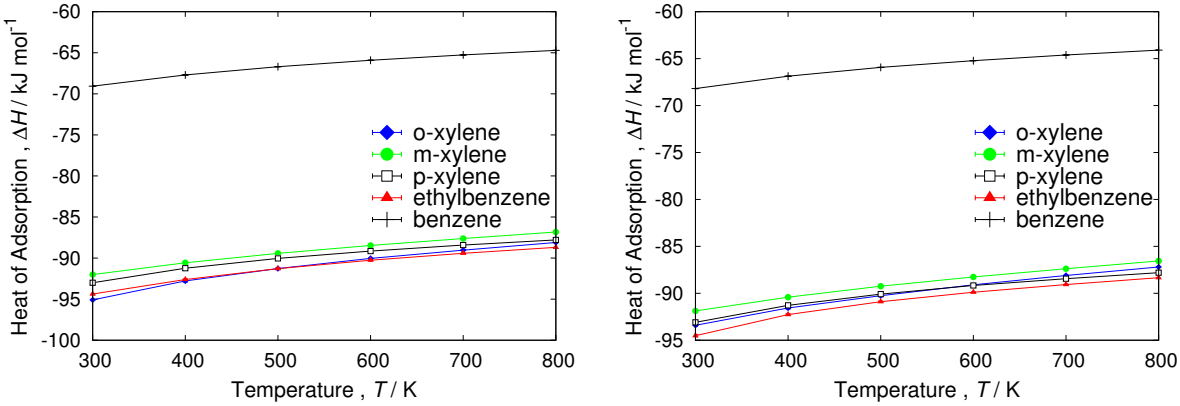

Figure S3: *Infinite dilution heat of adsorption of benzene, o-, m-, p-xylene and ethylbenzene in AFI (left) and MAZ (right) zeolites at different temperatures. For AFI zeolite, our results agree qualitatively with the experimental results of Chiang et al. [1]. In the Henry regime, benzene is the least strongly adsorbed species in both zeolites.*

4

Langmuir-Freundlich parameters for pure component aromatics at 433K in AFI

	site A			site B		
	$q_{i,A,\text{sat}}$ [molec. uc^{-1}]	$b_{i,A}$ [Pa$^{-\nu_{i,A}}$]	$\nu_{i,A}$ [-]	$q_{i,B,\text{sat}}$ [molec. uc^{-1}]	$b_{i,B}$ [Pa$^{-\nu_{i,B}}$]	$\nu_{i,B}$ [-]
o-xylene	0.402	7.63×10^{-7}	1	0.957	1.5×10^{-4}	1
m-xylene	0.208	1.26×10^{-7}	1	0.6935	0.6935×10^{-4}	1
p-xylene	0.277	5×10^{-7}	1	0.624	0.624×10^{-4}	1
ethylbenzene	0.208	3.18×10^{-7}	1	0.6935	0.6935×10^{-4}	1
benzene	0.2635	1.94×10^{-7}	1	1.123	1.123×10^{-5}	1
toluene	0.444	4.15×10^{-7}	1	0.929	0.929×10^{-5}	1

Table S1: *Dual-site Langmuir-Freundlich parameters for pure component xylene isomers at 433 K in AFI. The saturation capacities are expressed in molecules per unit cell; these numbers need to be multiplied by the conversion factor of 1.082 to get mol kg^{-1}.*

$$q_i = q_{i,A,sat} \frac{b_{i,A} f_i^{\nu_{i,A}}}{1 + b_{i,A} f_i^{\nu_{i,A}}} + q_{i,B,sat} \frac{b_{i,B} f_i^{\nu_{i,B}}}{1 + b_{i,B} f_i^{\nu_{i,B}}} \tag{4.1}$$

5

$Fe_2(BDP)_3$ variant

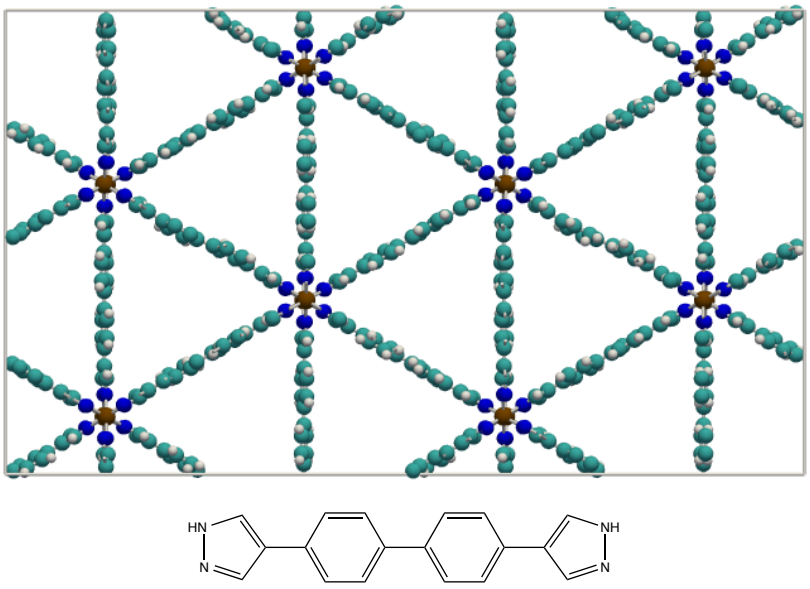

Figure S4: *$Fe_2(BDP)_3$ variant with a $4,4'-bis(1H-pyrazol-4-yl)$biphenyl instead of a BDP linker. The topology of the metal organic framework is the same as the $Fe_2(BDP)_3$, triangular 1D channels running in the z-direction, but the size of the channels is larger due to the extra aromatic molecule in the linker. Color code: organic linker (cyan), iron (brown), nitrogen (blue).*

6

Single component isotherms of trichlorobenzene isomers

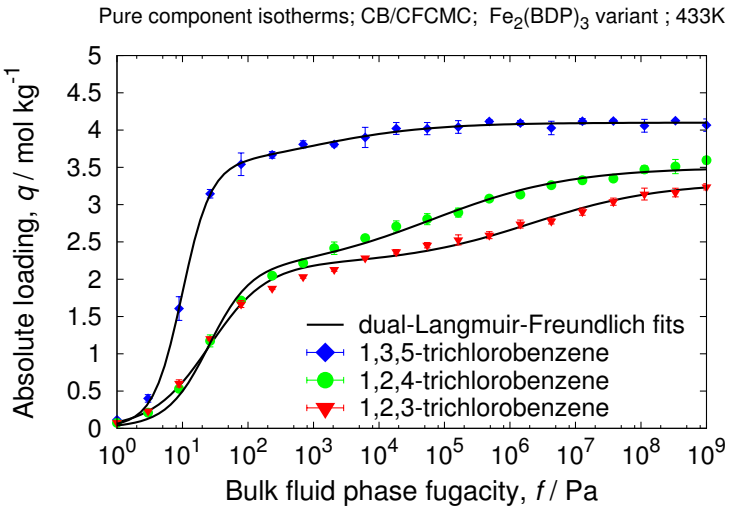

Figure S5: *Single component isotherms of 1,3,5-/1,2,4- and 1,2,3-trichlorobenzene in $Fe_2(BDP)_3$ variant at 433K. The 1,3,5-trichlorobenzene is the only isomer that can reorient within the metal-organic framework channels, which permits a higher saturation capacity.*

	site A			site B		
	$q_{i,A,\text{sat}}$ [mol. kg^{-1}]	$b_{i,A}$ [Pa$^{-\nu_{i,A}}$]	$\nu_{i,A}$ [-]	$q_{i,B,\text{sat}}$ [mol. kg^{-1}]	$b_{i,B}$ [Pa$^{-\nu_{i,B}}$]	$\nu_{i,B}$ [-]
1,3,5	3.45	1.03×10^{-2}	2	0.65	4.3×10^{-2}	0.47
1,2,4	1.4	1.07×10^{-2}	0.41	2.1	2.1×10^{-2}	1.38
1,2,3	1.1	1.64×10^{-3}	0.44	2.2	2.2×10^{-2}	1

Table S1: *Dual-site Langmuir-Freundlich parameters for pure component trichlorobenzene isomers at 433 K in $Fe_2(BDP)_3$ variant. The saturation capacities are expressed in mol kg^{-1}*

Bibliography

[1] A.S.T. Chiang, C.K. Lee, and Chang Z. H. *Zeolites*, 11:380, 1991.